Radiotherapy and Oncology 116 (2015) 462–466

Contents lists available at ScienceDirect

Radiotherapy and Oncology

journal homepage: www.thegreenjournal.com

Experimental radiobiology

Is there a causal relationship between genetic changes and radiomics-based image features? An *in vivo* preclinical experiment with doxycycline inducible GADD34 tumor cells

Kranthi Marella Panth *[,1], Ralph T.H. Leijenaar [1], Sara Carvalho, Natasja G. Lieuwes, Ala Yaromina, Ludwig Dubois, Philippe Lambin

Department of Radiation Oncology (MAASTRO), GROW, MUMC, Maastricht, The Netherlands

ARTICLE INFO

Article history:
Received 17 April 2015
Received in revised form 28 May 2015
Accepted 9 June 2015
Available online 7 July 2015

Keywords:
CT imaging
Radiogenomics
Preclinical
Radiotherapy

ABSTRACT

Background and purpose: The central hypothesis of "radiomics" is that imaging features reflect tumor phenotype and genotype. Until now only correlative studies have been performed. The main objective of our study is to determine whether a *causal relationship* exists between genetic changes and image features. The secondary objective is to assess whether the combination with radiotherapy (RT) influences these image features.

Material and methods: HCT116 doxycycline (dox) inducible GADD34 cells were grown as xenografts in the flanks of NMRI-nu mice. GADD34 overexpression decreases hypoxic fraction. Radiomics analyses were performed on computed tomography images obtained at 40 kVp and again at 80 kVp for validation, before radiotherapy at a volume of 200 mm^3, 4 days post RT (10 Gy) and 500 mm^3. To select reproducible features test–retest experiments were performed at baseline.

Results: Gene induction and/or irradiation translated into significant changes in radiomics features. Post irradiation, 17 features for 40 kVp and 9 features for 80 kVp differed significantly between dox+ and dox− combined with RT. 8 and 4 of these features remained consistent for 40 and 80 kVp, respectively.

Conclusion: Radiomics is able to identify early effects of changed gene expression combined with radiation treatment in tumors with similar volumes which are not visible to human eye.

Genomics and proteomics are widely used in the concept of personalized medicine [1,2]. However, tumor heterogeneity, which cannot be determined by invasive biopsies, varies spatially and temporally [3,4]. Advancements in medical imaging have provided better diagnostic biomarkers and novel imaging methods that can aid in early diagnosis, patient stratification and the monitoring of treatment responses [5]. Furthermore, three-dimensional tumor heterogeneity is defined by the underlying tumor genotype and phenotype. Therefore, the central hypothesis of radiomics is that features extracted from noninvasive images reflect the underlying phenotype and genotype [6]. Radiomics uses mathematical algorithms to extract a large number of quantitative features from medical images, describing tumor image intensity, shape and texture, capturing intra-tumoral heterogeneity [7] (http://www.radiomics.org; animation: https://youtu.be/Vf0F7q8vaS4).

It has previously been shown that radiomics can provide valuable information based on CT images [6,8] that have prognostic value in lung and head and neck cancer [7,9]. Segal has shown an association between defined imaging traits and gene expression profiles of human hepatocellular carcinomas (HCC) [10]. It was also reported that this radiogenomics approach can identify drug-responsive gene expression patterns in HCC [11]. In the context of radiomics, studies so far have shown only a correlation of the radiomics signatures to genetic signatures, but no causal relationship has been established.

The main goal of this study is to provide a proof-of-concept that genetic changes with phenotypic consequences influence image-derived radiomics features. More specifically, we prospectively evaluated whether radiomics features are causally related to genetic factors and whether radiation therapy affects those image features. In addition, we investigated whether the features obtained for all categories are reproducible in test–retest experiments and whether the features found remain consistent across

* Corresponding author at: Dept. of Radiation Oncology (Maastro Lab), Grow – School for Oncology and Developmental Biology, Maastricht University Medical Centre, Universiteitssingel 50/23, PO Box 616, 6200 MD Maastricht, The Netherlands.

E-mail address: kranthi.panth@maastrichtuniversity.nl (K.M. Panth).

[1] Indicates equal contribution.

http://dx.doi.org/10.1016/j.radonc.2015.06.013
0167-8140/

the different acquisition time points. Furthermore, we evaluated the effect of CT energy on radiomics features.

Materials and methods

Tumor cells and chemicals

Cells were cultured and maintained according to instructions and guidelines from the American Type Culture Collection. Doxycycline hyclate (dox) was purchased from Sigma Aldrich. Construction of HCT116 colorectal carcinoma cells overexpressing GADD34c and control pCDNA5(+) has been described previously [12].

Preclinical imaging studies

All animal experiments were approved by the Animal Ethical Committee of Maastricht University (2013-038). HCT116 tumor cells were subcutaneously injected in matrigel in the lateral flanks of NMRI-*nu*/*nu* mice. Mice were randomized after cell injection between doxycycline (dox+, $n = 17$) (2 g/L in 5% sucrose in drinking water) and placebo (dox−, $n = 16$) administration to induce expression of the gene of interest. HCT116 pCDNA5(+) xenografts were included to assess features related to dox administration without gene induction. CT images were obtained at two different energies (40 and 80 kVp) using the Precision X-ray X-RAD 225Cx at pre (baseline), at 4 days post radiation therapy (RT) and at a tumor volume of 500mm^3. The number of animals allocated per group after baseline scans was: dox+ RT- ($n = 8$), dox+ RT + ($n = 9$), dox− RT- ($n = 7$), dox− RT + ($n = 9$). Images were reconstructed with an isotropic voxel size of 0.1 mm. Tumors were irradiated with a single dose of 10 Gy at an average tumor volume of 210 (±36) mm^3. A second scan (retest) was acquired 5 min after the first (test) scan at baseline by repositioning the mouse in the scanner to determine feature test–retest (TRT) variability (Fig. 1).

Tumor delineation and image analysis

Tumors were delineated using SmART-Plan treatment planning software [13]. In order to acquire inter-observer variability (IOV), two experts independently delineated tumors from baseline images. For each image, we determined 625 radiomics features, grouped into five groups: (1) tumor intensity, (2) shape, (3) texture, (4) wavelet features, and (5) Laplacian of Gaussian (LoG) features. Features from group 1 describe the first-order histogram of all voxel intensity values in the tumor volume. Group 2 features describe the three-dimensional shape and size of a tumor. Features from group 3 quantify texture within the tumor image calculated from gray-level co-occurrence (GLCM), gray-level run-length (GLRLM), and gray-level size-zone texture matrices (GLSZM). Group 4 consists of features from group 1 and 2, after a wavelet decomposition of the image. Group 5 consists of features from group 1, calculated after applying Laplacian of Gaussian filtering to the image, highlighting image regions at different scales. Texture matrices were determined by considering 26 connected voxels (i.e. voxels were considered to be neighbors in all 13 directions in three dimensions) at a distance of 1 voxel. The features derived from GLCM and GLRLM were calculated by averaging their value over all 13 directions. LoG features were determined at a filter standard deviation ranging from 0.1 mm to 0.5 mm with 0.05 mm increments. Image analysis was performed in Matlab R2012b (The Mathworks, Natick, MA) using an adapted version of CERR [14] and Radiomics software developed in-house to extract imaging features. A detailed description and mathematical definitions of the radiomics features assessed in this study are described elsewhere [9,15].

Feature selection

The intra-class correlation coefficient (ICC) [16] was calculated to provide an indication of both the test–retest (TRT) and inter-observer (IOV) reliability of feature measurements. The ICC is a statistical measure between 0 and 1, where 0 indicates no reliability and 1 indicates perfect reliability. For the ICC regarding the TRT reliability of imaging features, we used the definition of ICC(1,1). The ICC for IOV was determined by the definition of ICC(2,1). To determine the ICCs, we obtained variance estimates by partitioning the total variance by means of analysis of variance (ANOVA). Absolute variability was furthermore estimated as the smallest detectible change (SDC) [17]. To provide a basis for evaluating the magnitude of the TRT and IOV SDC values, we determined a coefficient of reliability (COR) by normalizing SDC to a percentage of the range of feature values (2.5–97.5%) over all lesions included. For each feature, we determined the average TRT and IOV ICC rank and selected the resulting 50% top-ranked features for further analysis. We performed feature selection using R (version 3.1.0).

Statistical analyses

We performed a Wilcoxon rank sum test to compare feature values between two groups using R (version 3.1.0). We used a non-parametric *T*-test in Graphpad Prism v 5.03 to perform a statistical analysis to compare the tumor growth rates between the two groups. A *P*-value < 0.05 was considered significant.

Results

Upon GADD34 gene induction (dox+), no difference ($P = 0.405$) in tumor growth was observed compared to animals treated with

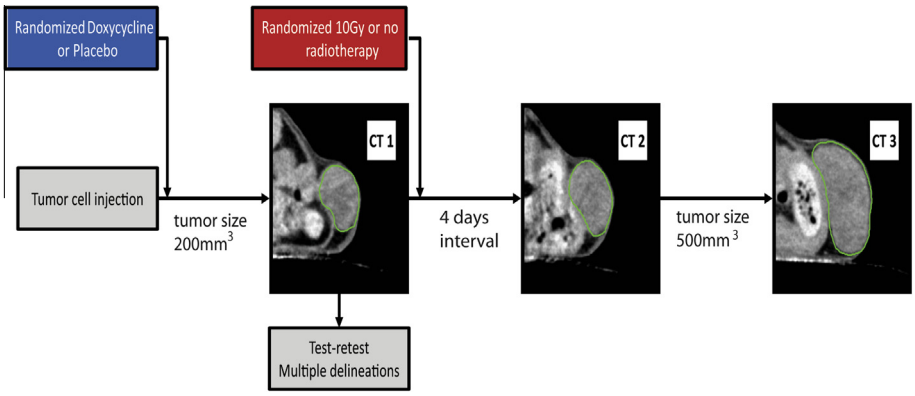

Fig. 1. Graphical representation of experimental work flow.

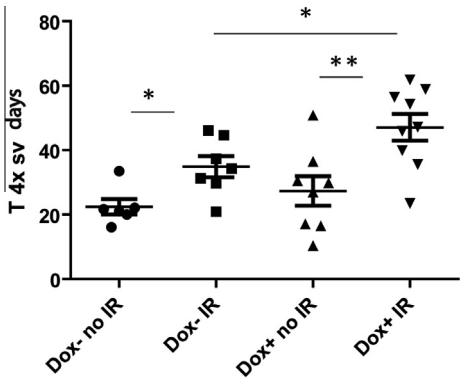

Fig. 2. Time to reach 4 times start volume (T4xSV) for the different treatment groups. $^{*}P < 0.05$, $^{**}P < 0.01$. Data represent the mean ± SD of at least 6 animals.

placebo (dox−). However, upon irradiation (single dose 10 Gy), the time to reach 4 times start volume for these doxycycline treated tumors was significantly ($P < 0.05$) increased upon irradiation (single dose 10 Gy) compared to dox− irradiated tumors (Fig. 2).

Image-derived quantitative features need to be robust and reproducible in order to provide reliable measurements. We therefore selected the 50% top-ranked features based on their average ICC for the TRT variability (ICC1) and inter-observer variability (ICC 2) (Fig. 3). In the control pCDNA5(+) group, 12 features were found to differ significantly ($P < 0.05$) between dox+ and dox− treatment groups. This suggests that these features were related to doxycycline administration. They were therefore eliminated in further analyses, which left 303 remaining features.

We first evaluated features from 40 kVp CT images for validating our hypothesis. We determined features that were significantly different between dox+ and dox− GADD34 tumors to investigate which image features are influenced by genetic factors. At a tumor volume of 200 mm^3 (baseline), 13 features (1 tumor intensity and 12 wavelet) were found to be significantly ($P < 0.05$) different. The second CT was acquired 4 days after baseline, the day animals were sham irradiated, and only 1 wavelet feature was observed to be different. At the third CT, at the final volume of 500 mm^3, 5 features (1 LoG and 4 wavelets) were significantly ($P < 0.05$) different (Fig. 4). However, these features were different across the three CT image time points. None of the features identified were correlated with tumor volume.

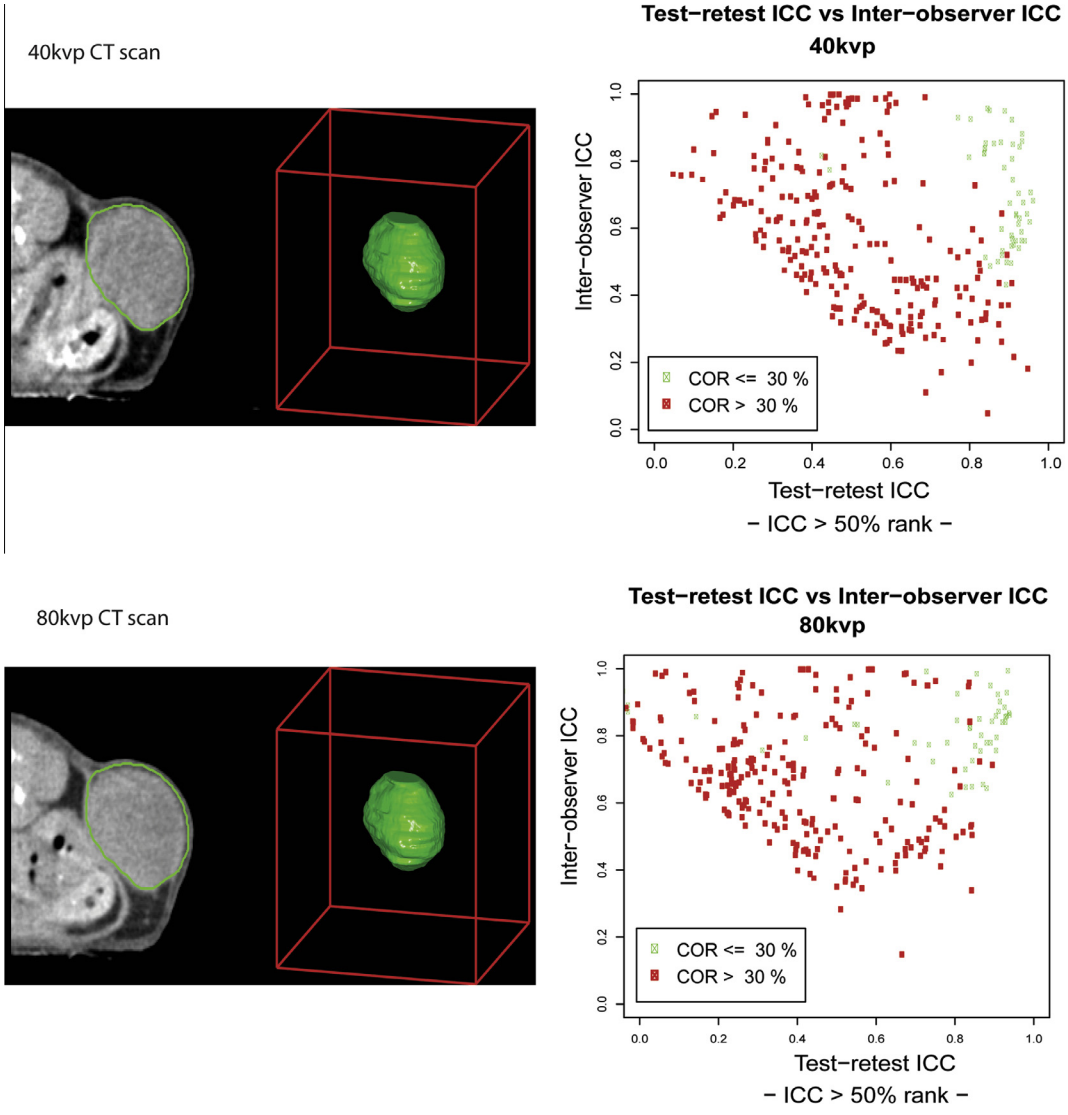

Fig. 3. Representative images of 40 kVp and 80 kVp energy CT and feature selection based on average ICC values of test–retest and inter-observer variability.

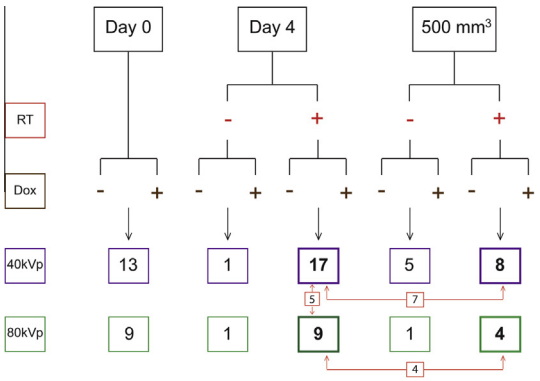

Fig. 4. Schematic representation of CT scan derived radiomic features (40 kVp purple and 80 kVp green) for different treatment groups at different time points. The numbers within the arrows show the number of features, which are consistent between the indicated imaging time points and different energies.

After RT (second CT acquisition), 17 features (3 tumor intensity and 15 wavelets) differed significantly ($P < 0.05$) between the dox+ group and dox− group. Five of those 17 features differed significantly ($P < 0.05$) between irradiated (RT+) and sham-irradiated (RT−) animals within the dox− group (3 tumor intensity and 2 wavelet). One feature ($P < 0.05$) (wavelet) differed between RT+ and RT− within the doxycycline-treated group (Supplementary Table 1). These 6 features are related to early effect of RT alone. At the final image acquisition time point, 8 features (wavelet) differed significantly ($P < 0.05$) between the dox+ and dox− groups. One of these 8 was found to be significantly different between RT+ vs RT− within dox− group derived at final time point. The remaining 7 features were consistent, since they were statistically different between the dox+ and dox− groups at both time points, 4 days post RT and at the final time point. These features were specific for the combination of RT with change in GADD34 gene expression (Fig. 4). Features found to be significantly different at all assessed time points after irradiation between dox+ and dox− groups were always consistently higher for dox+. An example is shown in Fig. 5A.

To further validate our findings, we obtained features from CTs performed at a higher energy level (80 kVp) (Fig. 3). At baseline, 9 features (1 tumor intensity, 1 gray-level intensity and 7 wavelet) were found to differ significantly between dox+ and dox− treatment groups. Similar to 40 kVp, these features lost significance at later time points. Upon RT, 9 features (wavelet) differed significantly between dox+ and dox−. Five of those features were also found in the 40 kVp CT images and out of which, one feature ($P < 0.05$) (wavelet) significantly differed between RT+ and RT− within the dox− group (Supplementary Table 2). The remaining 4 image features were also significantly different at later time points, but were not identified in the 40 kVp images (Fig. 4) (Supplementary Table 2). Similar to the 40 kVp obtained features, the 80 kVp image features were also consistently higher for dox+ than dox− at both imaging time points (Fig. 5B).

Discussion

Radiomics, an advanced analysis platform, extracts features from medical images by using mathematical algorithms based on tumor intensity, gray-level intensities, and texture [6–9,15,18–21]. We have previously identified radiomics-based signatures that are prognostic and associated with proliferation-related gene

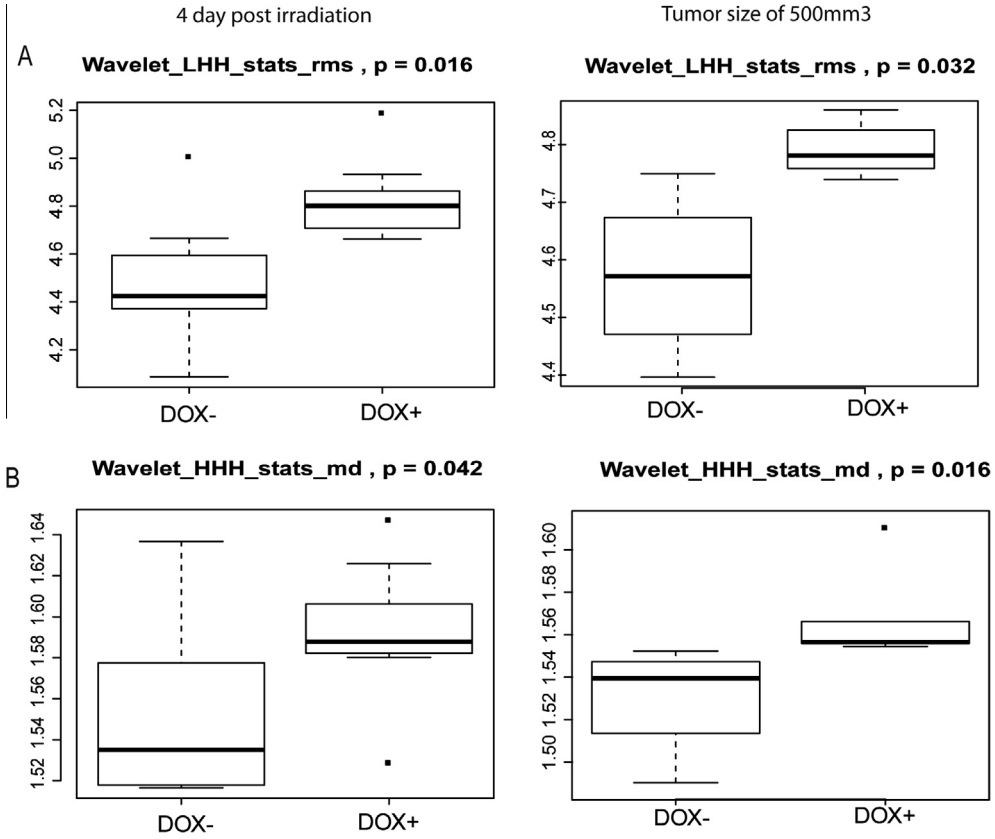

Fig. 5. Gene induction (dox+) results in significantly changed features compared to no gene induction (dox−) upon combination with radiotherapy 4 days after RT and at 500 mm^3. Features are extracted from 40 kVp (A) or 80 kVp (B) CT scans.

signatures [7]. Furthermore, radiogenomics imaging traits might act as molecular surrogates for predicting treatment responses [11]. The studies conducted so far on radiomics have only shown correlative association of radiomic signatures with gene signatures. In this preclinical radiogenomics study, we hypothesized that image features are *causally* related to genetic factors and that radiation affects these image features.

To prove our hypothesis, we first employed a genetic tumor model in which tumor microenvironmental characteristics like hypoxia change upon doxycycline administration [12]. We have previously demonstrated that tumoral GADD34 overexpression led to an inhibition of the eIF2α signaling pathway upon administration of doxycycline, resulting in decreased hypoxia tolerance and as a result reduced hypoxic fraction. Although this had no effect on tumor growth, a significantly enhanced growth delay was observed upon combination with tumor irradiation when compared with RT monotherapy [12]. Thus by employing this reproducible model under well-controlled experimental conditions, we could identify whether a change in GADD34 gene expression, is causally related with radiomics image features and whether this could be affected by radiation.

We have observed that a genetic change (dox+ vs dox− treatment group) results in significantly different radiomics features, although these features were not consistent across the different imaging time points. Next, certain radiomics features were significantly different upon RT monotherapy (RT− vs RT+ dox− treatment groups). Similar to genetic changes, features that differed significantly upon irradiation were not consistent between different CT acquisitions. This can be explained due to the dynamic changes in the tumor and tumor microenvironment over time. Along with tumor growth, necrotic fraction may also increase and hypoxic fraction may change. Post radiation therapy, neovasculature is formed; hypoxic repopulation occurs leading to intra-tumoral heterogeneity over time [22].

However, when GADD34 was induced and radiation therapy was given, there was additional growth delay due to a decreased hypoxic fraction at the time of irradiation, as previously described [12]. Thus the difference in tumor heterogeneity between gene-induced and non-induced tumors post RT was reflected in the imaging features likely as a result of a phenotypic change. Interestingly, the radiomics image features that were found to be significantly different between both groups shortly after irradiation were also observed at larger tumor volumes. This phenomenon was observed independent of the CT image acquisition energy level, although the observed features were different between both energies tested. Remarkably, the feature value for slow-growing tumors (gene-induced) was higher than for faster-growing tumors (no gene-induced group) upon combination with radiotherapy.

Conclusion

We have shown in *in vivo* preclinical models that radiomics is able to quantify the early effects of radiation treatment and genetic changes in tumors with similar volumes, and identify differences that are not visible to the human eye.

Conflict of interest

All authors declare that there are no conflicts of interest.

Acknowledgements

The authors acknowledge the support of the QuIC-ConCePT project, partly funded by EFPIA companies and the Innovative Medicine Initiative Joint Undertaking (IMI JU) under Grant Agreement No. 115151. The authors also acknowledge financial support from the National Institute of Health (NIH-USA U01 Radiomics), the EU 6th and 7th framework program (ARTFORCE) and Kankeronderzoekfonds Limburg from the Health Foundation.

Appendix A. Supplementary data

Supplementary data associated with this article can be found, in the online version, at http://dx.doi.org/10.1016/j.radonc.2015.06.013.

References

[1] Lambin P, van Stiphout RGPM, Starmans MHW, et al. Predicting outcomes in radiation oncology—multifactorial decision support systems. Nat Rev Clin Oncol 2013;10:27–40.
[2] Chin L, Andersen JN, Futreal PA. Cancer genomics: from discovery science to personalized medicine. Nat Med 2011;17:297–303.
[3] Lee S, de Boer WB, Fermoyle S, Platten M, Kumarasinghe MP. Human epidermal growth factor receptor 2 testing in gastric carcinoma: issues related to heterogeneity in biopsies and resections. Histopathology 2011;59:832–40.
[4] Ruijter ET, De Van, Kaa CA, Schalken JA, Debruyne FM, Ruiter DJ. Histological grade heterogeneity in multifocal prostate cancer. Biological and clinical implications. J Pathol 1996;180:295–9.
[5] Rudin M, Weissleder R. Molecular imaging in drug discovery and development. Nat Rev Drug Discov 2003;2:123–31.
[6] Lambin P, Rios-Velazquez E, Leijenaar R, et al. Radiomics: extracting more information from medical images using advanced feature analysis. Eur J Cancer 2012;48:441–6.
[7] Aerts HJWL, Velazquez ER, Leijenaar RTH. Decoding tumour phenotype by noninvasive imaging using a quantitative radiomics approach. Nat Commun 2014;5.
[8] Velazquez ER, Parmar C, Jermoumi M. Volumetric CT-based segmentation of NSCLC using 3D-Slicer. Sci Rep 2013;3.
[9] Coroller TP, Grossmann P, Hou Y, et al. CT-based radiomic signature predicts distant metastasis in lung adenocarcinoma. Radiother Oncol 2015;114:345–50.
[10] Segal E, Sirlin CB, Ooi C, et al. Decoding global gene expression programs in liver cancer by noninvasive imaging. Nat Biotech 2007;25:675–80.
[11] Kuo MD, Gollub J, Sirlin CB, Ooi C, Chen X. Radiogenomic analysis to identify imaging phenotypes associated with drug response gene expression programs in hepatocellular carcinoma. J Vasc Interv Radiol 2007;18:821–30.
[12] Rouschop KM, Dubois LJ, Keulers TG, et al. PERK/eIF2α signaling protects therapy resistant hypoxic cells through induction of glutathione synthesis and protection against ROS. Proc Natl Acad Sci 2013;110:4622–7.
[13] van Hoof SJ, Granton PV, Verhaegen F. Development and validation of a treatment planning system for small animal radiotherapy: SmART-Plan. Radiother Oncol 2013;109:361–6.
[14] Deasy JO, Blanco AI, Clark VH. CERR: a computational environment for radiotherapy research. Med Phys 2003;30:979–85.
[15] Leijenaar RTH, Carvalho S, Velazquez ER, et al. Stability of FDG-PET Radiomics features: an integrated analysis of test–retest and inter-observer variability. Acta Oncol 2013;52:1391–7.
[16] Shrout PE, Fleiss JL. Intraclass correlations: uses in assessing rater reliability. Psychol Bull 1979;86:420–8.
[17] Bland JM, Altman DG. Agreement between methods of measurement with multiple observations per individual. J Biopharm Stat 2007;17:571–82.
[18] Chicklore S, Goh V, Siddique M, Roy A, Marsden P, Cook GR. Quantifying tumour heterogeneity in 18F-FDG PET/CT imaging by texture analysis. Eur J Nucl Med Mol Imaging 2013;40:133–40.
[19] Parmar C, Rios Velazquez E, Leijenaar R, et al. Robust radiomics feature quantification using semiautomatic volumetric segmentation. PLoS ONE 2014;9:e102107.
[20] Kumar V, Gu Y, Basu S, et al. Radiomics: the process and the challenges. Magn Reson Imaging 2012;30:1234–48.
[21] Carvalho S, Leijenaar RTH, Velazquez ER, et al. Prognostic value of metabolic metrics extracted from baseline positron emission tomography images in non-small cell lung cancer. Acta Oncol 2013;52:1398–404.
[22] Moulder J, Rockwell S. Tumor hypoxia: its impact on cancer therapy. Cancer Metastasis Rev 1987;5:313–41.